# Reanalysis of the Extended Finite Element Method for Crack Initiation and Propagation

Matthew J. Pais[1], Nam-Ho Kim[2] and Timothy Davis[3]
*University of Florida, Gainesville, FL 32611*

**The extended finite element method allows one to represent strong (cracks) and weak (holes, material interfaces) discontinuities independent of the finite element mesh through the partition of unity. This allows one to avoid costly remeshing which occurs in the vicinity of the crack tip in the traditional finite element framework when modeling crack growth. However, fatigue crack growth simulation has been computationally challenging due to the large number of simulations needed to model growth to failure. Reanalysis techniques are well developed in the areas of design and optimization for the modification of the finite element stiffness matrix to account for the addition/modification of degrees of freedom as a result of the design change. In this paper, it is observed that modeling quasi-static crack growth in the extended finite element framework involves the addition of degrees of freedom to a system of equations. Therefore, a new reanalysis algorithm based on an incremental Cholesky factorization is introduced for modeling quasi-static crack growth in the extended finite element method. This method is also used to predict the angle of crack initiation using an optimization algorithm. The examples contained within show that a 30-48% reduction in the total computational time is achievable for using the reanalysis approach for solving optimization problems or modeling quasi-static growth. It is shown that the assembly time for the stiffness matrix is insensitive to the number of elements for the proposed method.**

## Nomenclature

| | | |
|---|---|---|
| $a$ | = | half crack length |
| $a_I$ , $b_I$ | = | enriched nodal degrees of freedom associated with enrichment functions |
| $h$ x | = | Heaviside enrichment function |
| $H$ $x$ | = | shifted Heaviside enrichment function |
| $r$ | = | distance from crack tip to a point of interest |
| $u^h$ $x$ | = | XFEM displacement approximation |
| $u_I$ | = | nodal degree of freedom vector associated with continuous finite element solution |
| $\theta$ | = | angle from crack to point of interest in the crack tip coordinate system |
| $\theta_c$ | = | angle of crack growth |
| $\phi_\alpha$ $x$ | = | linear elastic asymptotic crack tip enrichment function |
| $\Phi_\alpha$ x | = | shifted linear elastic asymptotic crack tip enrichment function |
| $\upsilon$ $x$ | = | generic enrichment function |
| $\upsilon_I$ $x$ | = | generic enrichment function evaluated at node $I$ of an element |

[1] Graduate Research Assistant, Department of Mechanical and Aerospace Engineering, PO Box 116250, Department of Mechanical and Aerospace Engineering, University of Florida, Gainesville, FL 32611-6250, Student Member.
[2] Associate Professor, Department of Mechanical and Aerospace Engineering, PO Box 116250, Department of Mechanical and Aerospace Engineering, University of Florida, Gainesville, FL 32611-6250, and AIAA Member.
[3] Professor, Computer and Information Science and Engineering, CISE Department, E301 CSE Building, University of Florida, PO Box 116120, Gainesville, FL 32611-6120.

$V(x)$ = enrichment function for voids

$\Upsilon\ x$ = generic shifted enrichment function

$\Omega$ = set of all nodes in the mesh

$\Omega_d$ = set of all enriched nodes

$\Omega_H$ = set of nodes whose shape function is cut by the crack

$\Omega_T$ = set of nodes whose shape functions are cut by the crack tip

## I. Introduction

MODELING crack growth in a traditional finite element framework is a challenging engineering task. Originally the finite element framework was modified to accommodate the discontinuities that are caused by phenomena such as cracks, inclusions and voids. The finite element framework is not well suited for modeling crack growth because the domain of interest is defined by the mesh. At each increment of crack growth, at least the domain surrounding the crack tip must be remeshed such that the updated crack geometry is accurately represented.

The extended finite element method (XFEM) along with the level set method can be used to alleviate many of the inconveniences of using the finite element method (FEM) to model the evolution of a crack. Special enrichment functions are added to the traditional finite element framework through the partition of unity framework[1]. For modeling the strong discontinuity of a cracked body two enrichment functions are used. The Heaviside step function represents the discontinuity away from the crack tip, and the linear elastic asymptotic crack tip displacement fields are used to account for discontinuity at the crack tip. The crack is represented independent of the mesh by the enrichment functions which allows for the crack geometry to be updated without a need to create/update a new mesh on the domain. For the case of a material interface, an enrichment function is used which combines distance from the weak discontinuity and the absolute value function.

Crack growth was modeled by combining the maximum circumferential stress criterion and Paris law for predicting the direction and incremental crack growth length. The stress intensity factors needed for these models were calculated using the domain form of the J-integral interaction integrals. Modeling crack growth is a computationally expensive task because it requires tens of thousands of loading cycles. Instead of performing a finite element analysis at each cycle, in the literature a fixed crack growth size[2] or a constant number of elapsed cycles[3] is used to approximate the total life of the component. This assumption yields a constant crack growth rate and direction for multiple cycles. As the direction of crack propagation can change in each cycle and as the rate of crack growth changes according to the crack size, this assumption does not yield the actual crack propagation path. In particular, Moës[2] showed different crack growth paths for different fixed crack growth sizes. In addition, it is not easy to estimate how many cycles will be needed for a given size of crack growth. In order to estimate accurate fatigue crack growth, it is necessary to perform a large number of analyses, which will be tremendously expensive.

Reanalysis algorithms[4,5] have been developed primarily for use in the fields of design and optimization to efficiently solve problems where small perturbations to the finite element domain are made. This may take the form of changing the location of elements, adding additional elements, or a combination of both. These methods can be classified as either being exact or approximate[6]. The exact methods are generally based on the Sherman-Morrison[7] inversion formula and consider cases where the modified elements affect a small number of degrees of freedom. The approximate methods are typically iteration based and are used when the modified elements affect a large number of degrees of freedom. Li and Wu[5,6,8] have introduced algorithms for the reanalysis of structures with added degrees of freedom through the use of an iterative solver. An exact reanalysis algorithm is used here to allow for each iteration of crack growth to be considered instead of using either a fixed increment of crack growth or number of cycles. The method is also used to reduce the cost of an optimization analysis of the angle of crack initiation for a crack emanating from a plate with a hole.

The organization of the paper is as follows. Section 2 reviews the basics of the extended finite element method along with the enrichment functions used for representing cracks and voids independent of the mesh. Section 3 reviews the crack growth model used in quasi-static analysis along with the contour integral formulation. Section 4 introduces the reanalysis algorithm using incremental Cholesky factorization. Section 5 first verifies the implementation of the enrichment functions for cracks and voids by comparison with benchmark problems. Then the reanalysis algorithm is explored through the use of a plate with an edge crack. Finally, the reanalysis algorithm is used to predict the location of crack initiation in a plate with a hole. For one of these cases, the crack is then grown to failure in over one thousand cycles and the resulting computational time for the brute force and reanalysis algorithm are compared.

## II. Extended Finite Element Method

The extended finite element method[2] (XFEM) allows discontinuities to be represented independent of the finite element mesh by exploiting the partition of unity finite element method[1] (PUFEM). Arbitrarily oriented discontinuities can be modeled independent of the finite element mesh by enriching all elements cut by a discontinuity using enrichment functions satisfying the discontinuous behavior and additional nodal degrees of freedom. In general the approximation of the displacement field in XFEM takes the following form:

$$\mathbf{u}^{\mathrm{h}}(x) = \sum_{I\in\Omega} \mathrm{N}_I(x)\left[\mathbf{u}_I + \sum_{I\in\Omega_d} \upsilon(x)\mathbf{a}_I\right] \tag{1}$$

where $\Omega$ is the entire domain and $\Omega_d$ is the domain containing discontinuities. In Eq. (1), $\mathrm{N}_I(x)$ are the traditional finite element shape function, $\upsilon(x)$ is the discontinuous enrichment function, and $\mathbf{u}_I$, $\mathbf{a}_I$ are the traditional and enriched degrees of freedom (DOF). Note that where $\Omega \bigcap \Omega_d = \varnothing$, the enrichment function $\upsilon(x)$ vanishes. As the discontinuities are not defined by the finite element mesh, the level set method[9,10] is used to track the discontinuities[11,12]. The approximation in Eq. (1) does not satisfy interpolation property; i.e., $\mathbf{u}_I \neq \mathbf{u}^h(x_I)$ due to enriched degrees of freedom. A common practice to satisfy the interpolation property in implementations of XFEM is to 'shift' the enrichment function[13] such that

$$\Upsilon_I(x) = \upsilon(x) - \upsilon_I(x)\,. \tag{2}$$

where $\Upsilon_I(x)$ is the shifted enrichment function for the i[th] node and $\upsilon_I(x)$ is the value of $\upsilon(x)$ at the i[th] node. Thus, the interpolation property is recovered as the shifted enrichment function $\Upsilon_I(x)$ vanishes at the node. Here lower case variables are used to represent the unshifted enrichment functions.

For modeling a crack in a homogeneous material, two different enrichment schemes are employed. For an element completely cut by a crack, the Heaviside[2] enrichment function is used such that

$$\mathrm{h}(x) = \begin{cases} +1 & \text{Above Crack} \\ -1 & \text{Below Crack} \end{cases}. \tag{3}$$

Thus a discontinuity is explicitly added to an element cut by a crack.

For the case of an element containing the crack tip, the asymptotic functions, originally introduced by Fleming[14] for the representing crack tip displacement fields in the element-free Galerkin (EFG) method and repeated by Belytschko,[15] are used in this paper. The near tip displacement field takes the form of the following four functions:

$$\phi_\alpha(x)\ _{\alpha=1-4} = \left\{\sqrt{r}\sin\frac{\theta}{2},\ \sqrt{r}\cos\frac{\theta}{2},\ \sqrt{r}\sin\theta\cos\frac{\theta}{2},\ \sqrt{r}\sin\theta\cos\frac{\theta}{2}\right\} \tag{4}$$

where $r$ and $\theta$ are the polar coordinates in the local crack-tip coordinate system. Note that the crack tip enrichment functions in Eq. (4) introduces a discontinuity across the crack in the element containing the tip, while the Heaviside function in Eq. (3) does in the elements cut by the crack. When a node would be enriched by both Eqs. (3) and (4), only Eq. (4) is used as is shown in Figure 1, in which the nodes with circle are enriched by Heaviside step function, and the nodes with square are by the crack tip enrichment functions.

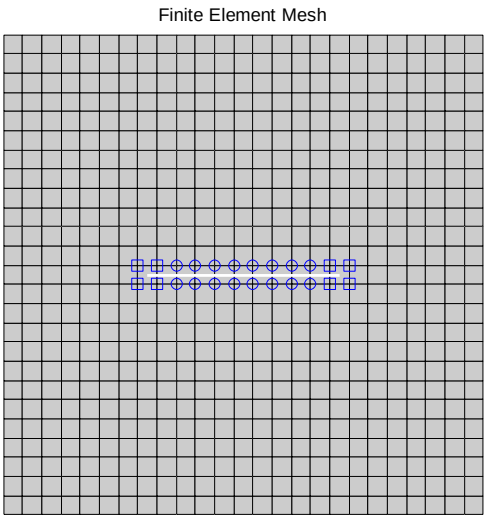


**Figure 1. The nodes enriched with the Heaviside (circle) and crack tip (square) enrichments.**

Voids[12,16] have been modeled independent of the finite element mesh using a different enrichment strategy which takes the form of

$$\mathbf{u}^h(x) = \mathrm{V}(x)\sum_{I\in\Omega} \mathrm{N}_I(x)\mathbf{u}_I \tag{5}$$

where $\mathrm{V}(x)$ is the void enrichment taking a value of zero inside the void and one outside the void. In two-dimensions, integration is performed only in the portion of an element containing material and nodes with support completely within in void are fixed. An example of the nodes which are fixed is shown in Figure 2. For more details on integration of an enriched element, the reader is referred to Mousavi[17] and Sukumar[18].

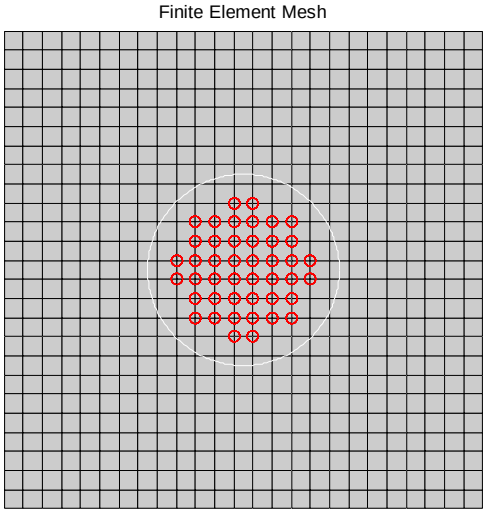


**Figure 2. The fixed degrees of freedom (red circles) associated with the hole enrichment.**

Using the Bubnov-Galerkin method to build the system of equations, we are able to derive a system of equations to represent the total domain where the approximation takes the following form:

$$\mathbf{u}^h(x) = \mathrm{V}(x)\sum_{I\in\Omega} \mathrm{N}_I(x)\left[\mathbf{u}_I + \sum_{I\in\Omega_{\mathrm{H}}} \mathrm{H}(x)\mathbf{a}_I + \sum_{I\in\Omega_{\mathrm{T}}}\sum_{\alpha=1}^{4} \Phi_\alpha(x)\mathbf{b}_I^\alpha\right] \tag{6}$$

where $\Omega_H$ is the domain cut by the crack, $\Omega_T$ is the domain containing the crack tip, $\mathrm{H}(x)$ is the shifted Heaviside enrichment and $\Phi_\alpha(x)$ is the shifted crack tip enrichment. The system of linear equation can be written in the form

$$\left[\mathbf{K}\right] \ \mathbf{u} \ = \ \mathbf{f} \tag{7}$$

where $\left[\mathbf{K}\right]$ is the global stiffness matrix, $\mathbf{u}$ are the global degrees of freedom and $\mathbf{f}$ are the applied loading. The elemental stiffness matrix is symmetric and takes the form

$$\mathbf{K}_e = \begin{bmatrix} \mathbf{K}_{uu} & \mathbf{K}_{ua} & \mathbf{K}_{ub} \\ \mathbf{K}_{ua}^T & \mathbf{K}_{aa} & \mathbf{K}_{ab} \\ \mathbf{K}_{ub}^T & \mathbf{K}_{ab}^T & \mathbf{K}_{bb} \end{bmatrix} \tag{8}$$

where $u$ refers to the traditional finite element stiffness values, $a$ refers to the Heaviside enrichment values and $b$ refers to the crack tip enrichment values and

$$\mathbf{K}_{\alpha\beta} = \int_\Omega \ \mathbf{B}_\alpha \ ^{\mathrm{T}} \mathbf{C} \mathbf{B}_\beta \mathrm{d}\Omega \qquad \alpha, \beta = u, a, b \ . \tag{9}$$

## III. Crack Growth Model

In order to determine how to propagate the crack, information is needed about the direction and magnitude of the crack growth at each growth increment. The direction of crack growth is found from the maximum circumferential stress criterion[19], which predicts that the crack will grow in the direction where $\sigma_{\theta\theta}$ is maximum. The angle of crack growth is given by

$$\theta_c = 2\arctan\frac{1}{4}\left(\frac{K_I}{K_{II}} - \mathrm{sign}\ \ K_{II}\ \sqrt{\left(\frac{K_I}{K_{II}}\right)^2 + 8}\right) \tag{10}$$

where $\theta_c$ is given in the crack tip coordinate system, and $K_I$ and $K_{II}$ are the mixed-mode stress intensity factors.

The Paris crack growth model[20] is used to determine the magnitude at which the crack will grow. For the through-thickness center crack in the infinite plate under Mode I loading, the Paris model takes the following form:

$$\frac{da}{dN} = C \ \ \Delta K \ ^m \tag{11}$$

where $da/dN$ is the crack growth rate, $\Delta K$ is the range of stress intensity factor. Although $N$ is an integer, it is considered as a real number because the crack growth is a slow process. By integrating Eq. (11), an equation for updating the crack length over $N$ cycles can be found such that

$$\Delta a = CN \ \ \Delta K \ ^m \tag{12}$$

where $\Delta a$ is the increment of crack growth. Note that the above equation is the forward finite different method, whose accuracy and stability are controlled by step size $N$. In many applications, the increment is very small as the crack grows over tens of thousands of cycles. Because the original Paris model is defined for the case of pure Mode I loading, the relationship proposed by Tanaka[21] is used to find the effective $\Delta K$ for the case of mixed-mode loadings.

$$\Delta K = \sqrt[4]{K_I^4 + 8K_{II}^4} \ . \tag{13}$$

The stress intensity factors needed for the maximum circumferential stress criterion and Paris model are calculated using the domain form of the interaction integrals[19,22]. For a general mixed-mode situation the relationship between the J-integral and the stress intensity factors can be given as

$$J = G = \frac{K_I^2}{E_{eff}} + \frac{K_{II}^2}{E_{eff}} \tag{14}$$

where $G$ is the energy release rate, and $E_{eff}$ is the effective Young's modulus, defined by a state of plane stress or plane strain as

$$E_{eff} = \begin{cases} E, & \text{Plane Stress} \\ \dfrac{E}{1-v^2}, & \text{Plane Strain} \end{cases} \tag{15}$$

where $E$ is Young's modulus and $v$ is Poisson's ratio. In order to calculate the mixed-mode stress intensity factors, an auxiliary stress state is superimposed onto the stress and displacement fields from the XFEM analysis. The auxiliary stress and displacement equations are chosen to be those derived by Westergaard[23] and Williams[24] which are given in the Appendix. The XFEM solutions are denoted with superscript (1) as $\sigma_{ij}^{\ 1}$ , $\varepsilon_{ij}^{\ 1}$ and $u_i^{\ 1}$ , while that from the auxiliary state as $\sigma_{ij}^{\ 2}$ , $\varepsilon_{ij}^{\ 2}$ and $u_i^{\ 2}$ .

Recall that the J-integral[25] takes the form of

$$J_i = \int_\Gamma \left[ W n_i - \sigma_{jk} n_j \frac{\partial u_k}{\partial x_i} \right] d\Gamma \tag{16}$$

where $W$ is the strain energy density and $i$ denotes the crack tip opening direction, which is assumed to correspond to the global x-direction, denoted $x_1$. The summation convention is used for the repeated indices. Equation (16) can be rewritten into a more convenient form as

$$J_1 = \int_\Gamma \left[ W\delta_{1j} - \sigma_{ij} \frac{\partial u_i}{\partial x_1} \right] n_j d\Gamma \,. \tag{17}$$

The two stress states can be superimposed into Eq. (17) such that

$$J_1^{(1+2)} = \int_\Gamma \left[ \frac{1}{2} \left( \sigma_{ij}^{\ 1} + \sigma_{ij}^{\ 2} \right) \left( \varepsilon_{ij}^{\ 1} + \varepsilon_{ij}^{\ 2} \right) \delta_{1j} - \left( \sigma_{ij}^{\ 1} + \sigma_{ij}^{\ 2} \right) \frac{\partial \left( u_i^{\ 1} + u_i^{\ 2} \right)}{\partial x_1} \right] n_j d\Gamma \,. \tag{18}$$

The J-integrals for pure state 1 and auxiliary state 2 can be separated from Eq. (18), which leaves an interaction term such that

$$J_1^{\ 1+2} = J_1^{\ 1} + J_1^{\ 2} + I^{\ 1,2} \tag{19}$$

where $I^{\ 1,2}$ is the interaction term and is given by

$$I^{\ 1,2} = \int_\Gamma \left[ W^{\ 1,2} \delta_{1j} - \sigma_{ij}^{\ 1} \frac{\partial u_i^{\ 2}}{\partial x_1} - \sigma_{ij}^{\ 2} \frac{\partial u_i^{\ 1}}{\partial x_1} \right] n_j d\Gamma \tag{20}$$

where $W^{1,2}$ is the interaction strain energy density

$$W^{1,2} = \sigma_{ij}^{1}\,\varepsilon_{ij}^{2} = \sigma_{ij}^{2}\,\varepsilon_{ij}^{1}\,. \tag{21}$$

Since we are superimposing two cracked configurations onto one another we can also write Eq. (14) as

$$J_1^{1+2} = \frac{\left(K_I^{1} + K_I^{2}\right)^2}{E_{eff}} + \frac{\left(K_{II}^{1} + K_{II}^{2}\right)^2}{E_{eff}}. \tag{22}$$

Expanding and rearranging terms from Eq. (22) yields

$$J_1^{1+2} = J_1^{1} + J_1^{2} + \frac{2\,K_I^{1}\,K_I^{2} + K_{II}^{1}\,K_{II}^{2}}{E_{eff}}. \tag{23}$$

Setting Eq. (19) and Eq. (23) equal leads to the relationship

$$I^{1,2} = \frac{2\,K_I^{1}\,K_I^{2} + K_{II}^{1}\,K_{II}^{2}}{E_{eff}}. \tag{24}$$

The stress intensity factors for the current state can be found by separating the two modes of fracture. By selecting $K_I^{2} = 1$ and $K_{II}^{2} = 0$, we are able to solve for $K_I^{1}$ such that

$$K_I^{1} = \frac{2I^{1,\text{Mode I}}}{E_{eff}}. \tag{25}$$

A similar procedure can also be followed such that $K_{II}^{1}$ is given by

$$K_{II}^{1} = \frac{2I^{1,\text{Mode II}}}{E_{eff}}. \tag{26}$$

The contour defining $I^{1,2}$ is converted to an area integral by using a smoothing function $q$. This function takes a value of one on the innermost contour and a value of zero on the outermost contour. At any point in the area integral, the linear shape functions are used to interpolate the value of $q$. The area integral is chosen to be a circular domain about the crack tip. With sufficiently large radius, the contour integral becomes path independent. This value was determined to correspond to a radius of three. The divergence theorem can be used to give the following equation for the domain form of the interaction integral:

$$I^{1,2} = \int_A \left[\sigma_{ij}^{1}\,\frac{\partial u_i^2}{\partial x_1} - \sigma_{ij}^{2}\,\frac{\partial u_i^1}{\partial x_1} - W^{1,2}\,\delta_{1j}\right]\frac{\partial q}{\partial x_j}\,\mathrm{d}A \tag{27}$$

## IV. Reanalysis

Recall that the approximation of the displacement in XFEM takes the form

$$u^h(x) = \sum_I N_I(x)\left[u_I + H_I(x)\,a_I + \sum_{\alpha=1}^{4}\Phi_\alpha(x)\,b_I^\alpha\right] \tag{28}$$

and the corresponding finite element stiffness matrix takes the form

$$K = \begin{bmatrix} K_{uu} & K_{ua} & K_{ub} \\ K_{ua}^T & K_{aa} & K_{ab} \\ K_{ub}^T & K_{ab}^T & K_{bb} \end{bmatrix}. \tag{29}$$

It can be noticed from Eq. (28) that the stiffness component associated with the traditional finite element approximation is not a function of the crack location, which implies that the $K_{uu}$ component of the stiffness matrix will be constant at each iteration of crack growth. This implies that the changing portion of the stiffness matrix is the enriched portion, which will be small compared to the un-enriched portion. Furthermore, it can also be noticed that while the Heaviside enrichment term is a function of the crack location within an element, that once an element has been enriched with the Heaviside enrichment its stiffness value will not change in any future iterations, meaning that the stiffness components containing subscript *a* will be constant for future iterations of crack growth.

Thus it is only necessary to consider elements which convert from a crack tip enrichment to a Heaviside enrichment as a result of crack growth and new elements containing crack tips at each iteration after the initial iteration. If an incremental crack growth, $\Delta a$, which is less than the elemental length is considered, then for any iteration after the initial iteration the stiffness matrix in only about 10 elements per tip must be considered instead of the entire domain. This clearly leads to a drastic decrease in the computational time required for the simulation of crack growth in the XFEM environment.

Further increases in reducing computational time may be achieved by considering an incremental Cholesky factorization of the global stiffness matrix. This algorithm is based on the realization that the crack exists in a relatively small area of the total domain being modeled. Furthermore, of the enriched domain, a large amount of the domain can be considered to be constant as the result of the Heaviside enrichment. Recall that the Cholesky factorization of a matrix $A$ takes the form[26]

$$A = \begin{bmatrix} A_{11} & A_{12} \\ A_{12}^T & A_{22} \end{bmatrix} = \begin{bmatrix} L_{11} & 0 \\ L_{21} & L_{22} \end{bmatrix} \begin{bmatrix} L_{11}^T & L_{21}^T \\ 0 & L_{22}^T \end{bmatrix} = LL^T. \tag{30}$$

where

$$\begin{aligned} L_{11} &= chol\ \ A_{11} \\ L_{21}^T &= L_{11} \backslash A_{12} \\ L_{22} &= chol\ \ A_{22} - L_{21} L_{21}^T \end{aligned} \quad . \tag{31}$$

With the above algorithm, $A_{11}$ can be considered to be equivalent to

$$A_{11} = \begin{bmatrix} K_{uu} & K_{ua} \\ K_{ua}^T & K_{aa} \end{bmatrix} \tag{32}$$

in the first iteration. Due to crack growth, the submatrices $A_{12}$ and $A_{22}$ in Eq. (30) will be modified. The components of the global stiffness matrix associated with the crack tip can be considered as

$$A_{12} = \begin{bmatrix} K_{ub} \\ K_{ab} \end{bmatrix}, \quad A_{22} = K_{bb}. \tag{33}$$

Then $A_{11}$ can be kept and reused at future iterations of crack growth. Then the above algorithm can be used to find the factorization for the new constant stiffness matrix components as a result of new Heaviside nodes. The new factorization can be appended to the end of the previous iteration's $A_{11}$, then Eqs. (31) and (33) can be used to factor the new crack tip stiffness matrix. This method can save the Cholesky factorization of the entire stiffness matrix, which takes the most computational cost in finite element analysis. However, it requires more information from the matrix solver, such as internal reordering sequences. Thus, when a matrix solver allows accessing this information, then Eq. (30) can be used to modify the factorized matrix.

Due to limitations in sparse division present within MATLAB, the above algorithm has not been implemented in this work. Instead the global stiffness matrix is modified at each increment and factored from scratch within MATLAB. Figure 3 illustrates the portion of stiffness matrix that is kept constant from the previous iteration and the other portion that has to be modified due to crack growth. Although this method requires factorization of the entire stiffness matrix, it can still save matrix assembly time. Example D in Section V shows that this can save computational cost up to 48%. An iterative procedure such as the one introduce by Wu[5] could also be used to solve the system of equations.

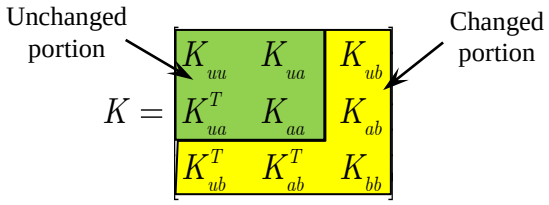


**Figure 3. Reanalysis of XFEM stiffness matrix due to crack growth.**

## V. Numerical Results

To verify the implementation of XFEM and the domain form of the J-integrals, three test cases are presented before the problem of interest is investigated further. The last example demonstrates crack initiation and propagation in the plate with a hole. All example problems were run on a Pentium 4 3.0 GHz computer with 4 GB of memory on MATLAB R2009a installed on the Windows XP 64 bit operating system.

### A. Center Crack in an Infinite Plate under Tension

For a center crack in an infinite plate under tension the theoretical stress intensity factor[27] takes the following form:

$$K_I = \sigma\sqrt{\pi a} \tag{34}$$

where $\sigma$ is the applied nominal stress and $a$ is the half crack length. Half of the domain is modeled and symmetric boundary conditions are applied. The initial half crack length is 1 m, and unit tension is applied at the top and bottom surface of the domain, defining the theoretical stress intensity factor to be 1.77. An aluminum alloy with E = 70 GPa and v = 0.3 and a half domain of size 15 m by 30 m was modeled with square quadrilateral 4 node elements of size h = 0.01 giving a calculated stress intensity factor of 1.78. Thus, the XFEM can predict the stress intensity factor with error in 0.5%.

### B. Inclined Crack in an Infinite Plate under Tension

For an inclined center crack in an infinite plate under tension the theoretical mixed-mode stress intensity factors[27] take the form

$$\begin{aligned} K_I &= \sigma\sqrt{\pi a}\cos^2\beta \\ K_{II} &= \sigma\sqrt{\pi a}\cos\beta\sin\beta \end{aligned} \tag{35}$$

where $\beta$ is the angle of inclination from the positive x-axis. A half crack length of 1 m and 1 N tension are applied to the domain. An aluminum alloy with E = 70 GPa and v = 0.3 and a domain of size 30 by 30 was modeled with square quadrilateral 4 node elements of size h = 0.005. Angles of inclination $\beta$ are chosen to be 15°, 30° and 45°. The results are summarized in Table 1.

**Table 1. Comparison of mixed-mode stress intensity factors for several angles of inclination.**

| | Theoretical | | Calculated | | Percent Error | |
|---|---|---|---|---|---|---|
| B | $K_I$ | $K_{II}$ | $K_I$ | $K_{II}$ | $K_I$ | $K_{II}$ |
| 15 | 1.65 | 0.44 | 1.63 | 0.42 | 1.2 | 4.5 |
| | | | | | | |
| 30 | 1.33 | 0.77 | 1.34 | 0.75 | 0.8 | 2.6 |
| | | | | | | |
| 45 | 0.89 | 0.89 | 0.88 | 0.86 | 1.1 | 3.3 |

### C. Hole in an Infinite Plate under Tension

To verify the XFEM void implementation a plate with a circular hole is considered. A plate of size 10 m x 10 m was modeled with a center hole with radius 0.4 m under unit tension in the y-direction with square four node quadrilateral elements of element size 0.0025. The theoretical values[28] for this case are given as

$$\begin{aligned}
\sigma_{xx}\ r,\theta &= -\frac{a^2}{r^2}\ \frac{1}{2}\ \cos 2\theta - \cos 4\theta\ \ - \frac{3}{2}\frac{a^4}{r^4}\cos 4\theta \\
\sigma_{yy}\ r,\theta &= 1 - \frac{a^2}{r^2}\ \frac{3}{2}\ \cos 2\theta + \cos 4\theta\ \ + \frac{3}{2}\frac{a^4}{r^4}\cos 4\theta \\
\sigma_{xy}\ r,\theta &= -\frac{a^2}{r^2}\ \frac{1}{2}\ \sin 2\theta + \sin 4\theta\ \ + \frac{3}{2}\frac{a^4}{r^4}\sin 4\theta
\end{aligned} \tag{36}$$

where $r$ and $\theta$ are polar coordinates from the center of the circle and $a$ is the hole radius. The resulting theoretical and numerical stress contours for $\sigma_{yy}$ are shown in Figure 4 and are in good agreement. The higher stress concentration values in the XFEM solution are likely due to there being a small lingering finite plate effect leading to an increase in the calculated stress values. This enrichment scheme was shown by Sukumar[12] to converge at a rate comparable to traditional FEM.

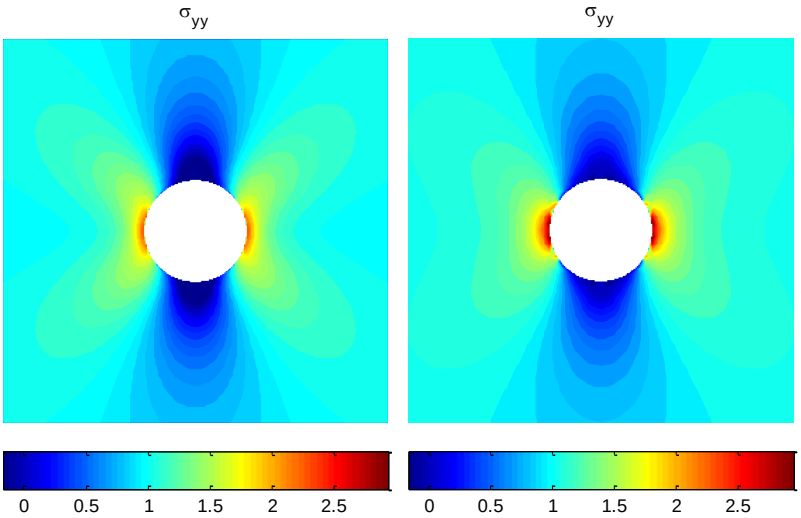


**Figure 4. The stress contour for a plate with hole under unit tension, theoretical (left) and calculated (right).**

### D. Analysis of Reanalysis Algorithm

The problem which will be given a detailed discussion here is that of an edge crack under uniaxial tension as shown in Figure 5.

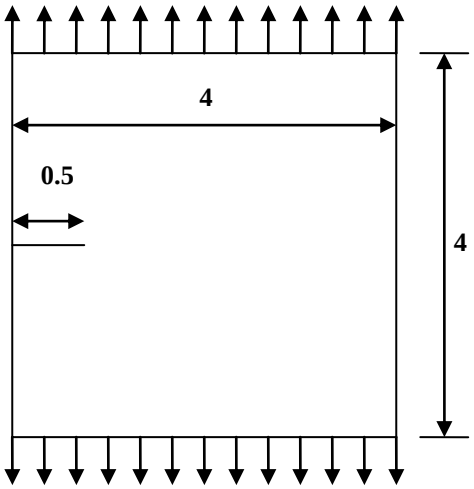


**Figure 5. The edge cracked specimen and loading of interest for the reanalysis benchmark.**

The first test was to perform 30 iterations of crack growth with a constant crack growth increment of 0.1 and square quadrilateral elements with sides of length 1/15. The total computational time for the case without reanalysis was 83 seconds, while the total time with reanalysis was 43 seconds.

For a more detailed analysis, the time for assembling the stiffness matrix as a function of iteration was considered. The results are shown in Figure 6. Note that in addition to a drastic decrease in computational time for the assembly of the stiffness matrix that the reanalysis algorithm is significantly less sensitive to the increasing number of degrees of freedom caused by the additional elements containing enriched degrees of freedom than the original method by itself.

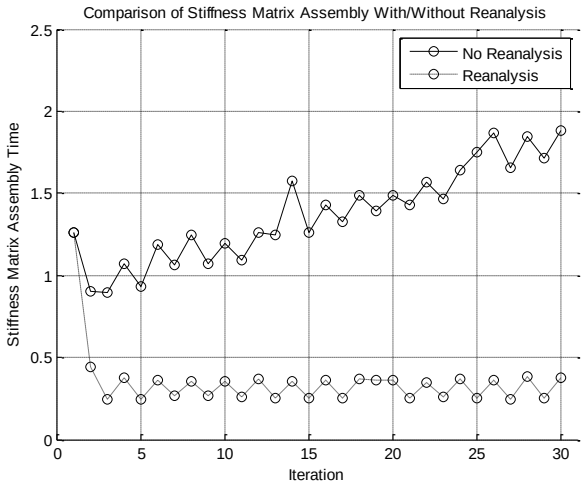


**Figure 6. Comparison of stiffness matrix assembly with and without reanalysis.**

A study was also done where only two iterations were performed on the geometry presented in Figure 5. Here the goal was to determine how sensitive the cost of reanalysis is to that of the mesh density. The increment of crack growth at each increment was chosen to be equal to the elemental length such that each case would experience approximately the same change in the total number of degrees of freedom in the system of equations. These results are summarized in Figure 7.

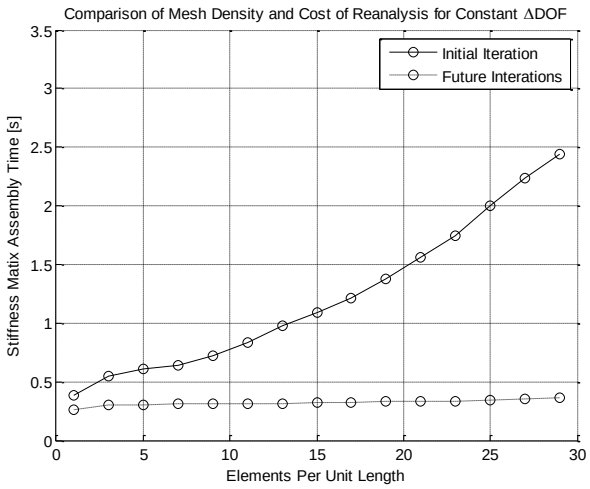


**Figure 7. Comparison of mesh density to cost of reanalysis for constant $\Delta \mathrm{DOF}$.**

There are several observations which one can make from Figure 7. The first is that while the cost of building the finite element stiffness matrix is approximately quadratic with respect to the mesh density for the structured mesh used, the cost for updating is almost constant. Note that the slightly higher costs for 10, 20 and 30 elements per unit length are a function of the crack tip being at an element edge and therefore, additional elements are considered in the crack tip enrichment. Also, the relative cost of updating versus the initial iteration's cost decreases drastically with mesh density. Thus, if the cost for solving the system of equations for a more dense mesh is not too large, there is no reason not to use a more dense mesh when considering modeling crack growth.

While the results from Figure 7 are true for a constant change in number of additional degrees of freedom, a more accurate representation of the modeling would be to consider the same crack growth increment for all mesh densities, which leads to an increased amount of updating as the mesh density decreases. These results are shown in Figure 8.

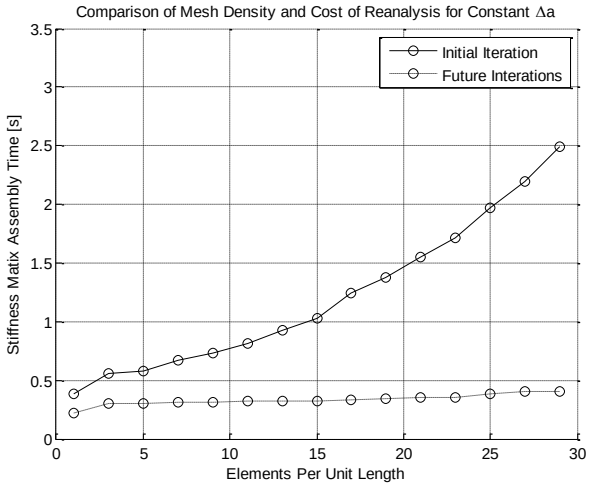


**Figure 8. Comparison of mesh density to cost of reanalysis for constant $\Delta a$.**

The very encouraging results from Figure 8 show very similar results to those in Figure 7. The reanalysis is a bit more expensive, but still nearly linear and still much less expensive than the initial iteration.

### E. Crack Initiation and Growth from a Plate with a Hole

The proposed example problem to be considered is that of a plate with a hole. A crack will be assumed to initiate and then propagate from some location at the interface of the hole. As this point will be unknown, numerous initial

cracks will be considered of small length and normal to the hole at single degree increments about the full radius of the hole. The point(s) with the largest stress intensity factor will be used as the initial crack location and the crack will propagate under quasi-static conditions to failure from exceeding the critical stress intensity factor for the given material. Every cycle will be considered, unlike previous crack growth simulations.

The optimization problem takes the following form for this problem:

$$\begin{aligned} &\min -G \\ &\text{s.t.} \quad \frac{\pi}{2} \le \theta \le \frac{3\pi}{2} \end{aligned} \tag{37}$$

where $G$ is given by Eq. (14) and $\theta$ is the angle that the crack makes with the positive x-axis as shown in . Due to the direction of the applied shear τ only the left side of the hole is considered for the optimization. The chosen material properties are those of Al 7075, which are E = 71.7 GPa, $\upsilon$ = 0.33 and $K_{IC}$ = 30 MPa.

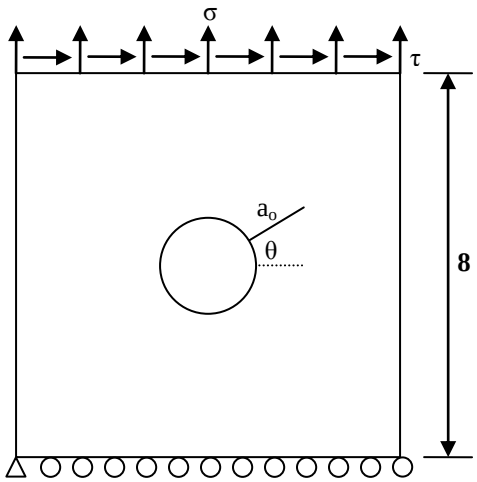


**Figure 9. Geometry used for the initiation and growth of a crack from a hole in a plate.**

Various tensile σ and shear τ loading combinations are applied to the given geometry to define the effect of the angle of crack initiation. The plate of size 8 x 8 m and structured mesh with elemental length of 0.05 which corresponds to about 52,000 degrees of freedom depending upon the orientation of the initial crack was used in the optimization. The *fminbnd* command within MATLAB was used for the optimization with tolerances on $G$ and $\theta$ of 1E-9 and 1E-6 respectively. For the optimization algorithm the reanalysis algorithm presented in Section IV is used, except here all enriched components of the stiffness matrix are calculated at each iteration as no portions are constant. The resulting optimum angles based on the applied loading ratio is given in Table 2.

**Table 2. Crack initiation angle and comparison between brute force and reanalysis algorithms.**

| Tension | Shear | Theta [rad] | Iterations | Brute Force [s] | Reanalysis [s] | Difference [%] |
|---|---|---|---|---|---|---|
| 0 | 1 | 3.14 | 28 | 392 | 301 | 23 |
| 1 | 0 | 2.41 | 28 | 394 | 302 | 23 |
| 1 | 1 | 2.58 | 31 | 434 | 305 | 30 |
| 1 | 5 | 2.90 | 32 | 448 | 293 | 35 |
| 1 | 10 | 2.90 | 31 | 434 | 297 | 32 |
| 5 | 1 | 2.44 | 31 | 433 | 336 | 23 |
| 10 | 1 | 2.41 | 27 | 378 | 293 | 23 |

The geometry with equivalent shear and tensile loading is used for to illustrate the advantages of the applied method with respect to modeling quasi-static growth. The initial crack of length 0.15 m is grown to failure, ie. when the equivalent stress intensity factor given by Eq. (13) is equal to the materials critical stress intensity factor. The loading is increased for both tension and shear to 1E6. Here each iteration of crack growth it simulated until failure occurs. In each case, failure occurs at 1337 iterations of growth with an approximate crack length of 0.193 m.

At this point in time the total time for the brute force method was 18734 seconds while for the reanalysis algorithm the total time was 12711 seconds. If each iteration is compared we find that the average time per iteration was 14.0 seconds, while the reanalysis algorithm was 9.5 seconds. This is approximately a savings of 32% compared to the traditional method and clearly illustrates the advantages of the proposed method when compared to the traditional methods.

Note that the crack fails before growing though a substantial number of elements. Therefore, the total number of degrees of freedom does not change significantly between the initial and final iteration for this examples. By comparison, Example D shows a large change in the number of degrees of freedom and correspondingly a larger amount of savings compared to the traditional method.

## VI. Conclusions and Future Plans

A reanalysis algorithm for the extended finite element method has been introduced. This method allows one to model in a more efficient manner problems where the geometry is constant, while the location of some or all of the discontinuities is not constant between iterations. This algorithm allows for optimization problems to be explored which may have previously have been too expensive. Furthermore, great savings in computational time can be achieved when the algorithm is used for modeling quasi-static growth. The savings from using the proposed method allow for problems to be solved which may have not been feasible prior to the introduction of this method. While a simple solution procedure has been used here which does not take advantage of the repeated factorization of a large portion of the stiffness matrix, large gains in computational time have been achieved. With the use of an incremental Cholesky factorization or other reanalysis technique which does not require for a repeated factorization of the constant components of the stiffness matrix further savings for both the optimization and quasi-static problem may be achieved. It was shown that reductions of up to 35% in simulation time can be achieved when the reanalysis algorithm is used for optimization problems. As the number of iterations would increase, these savings would also increase. It was shown that for the considered optimization problem, up to a 35% reduction in savings could be achieved by using the reanalysis algorithm. For the case of quasi-static crack growth, it was shown that for a case where the total number of degrees of freedom is not significantly different from the initial and final iteration a savings of about 30% could be achieved. As the number of degrees of freedom added to the system of equations during the analysis increases, additional savings are obtained using the reanalysis algorithm instead of the traditional approach. One area where the proposed method may be applied is to the modeling of crack growth in a structure with non-cyclic loading. In this case, the assumption of a constant increment of crack growth or cycles does not hold and each individual cycle of loading must be modeled. The proposed method greatly alleviates solving problems of this type.

## Appendix

The auxiliary stresses derived by Westergaard[23] and Williams[24] are

$$\sigma_{11} = \frac{1}{\sqrt{2\pi r}} \; K_I \cos\frac{\theta}{2}\left[1 - \sin\frac{\theta}{2}\sin\frac{3\theta}{2}\right] - K_{II}\sin\frac{\theta}{2}\left[2 + \cos\frac{\theta}{2}\cos\frac{3\theta}{2}\right] \tag{A1}$$

$$\sigma_{22} = \frac{1}{\sqrt{2\pi r}} \; K_I \cos\frac{\theta}{2}\left[1 + \sin\frac{\theta}{2}\sin\frac{3\theta}{2}\right] + K_{II}\sin\frac{\theta}{2}\cos\frac{\theta}{2}\cos\frac{3\theta}{2} \tag{A2}$$

$$\sigma_{33} = \upsilon \; \sigma_{11} + \sigma_{22} \tag{A3}$$

$$\sigma_{23} = \frac{1}{\sqrt{2\pi r}} K_{III}\cos\frac{\theta}{2} \tag{A4}$$

$$\sigma_{31} = \frac{-1}{\sqrt{2\pi r}}\sin\frac{\theta}{2} \tag{A5}$$

$$\sigma_{12} = \frac{1}{\sqrt{2\pi r}} \; K_I \sin\frac{\theta}{2}\cos\frac{\theta}{2}\cos\frac{3\theta}{2} + K_{II}\cos\frac{\theta}{2}\left[1 - \sin\frac{\theta}{2}\sin\frac{3\theta}{2}\right] \tag{A6}$$

and the auxiliary displacements are

$$u_1 = \frac{1}{2\mu}\sqrt{\frac{r}{2\pi}} \quad K_I \cos\frac{\theta}{2} \ \kappa - \cos\theta \ \ + K_{II} \sin\frac{\theta}{2} \ \kappa + 2 + \cos\theta \tag{A7}$$

$$u_2 = \frac{1}{2\mu}\sqrt{\frac{r}{2\pi}} \quad K_I \sin\frac{\theta}{2} \ \kappa - \sin\theta \ \ + K_{II} \cos\frac{\theta}{2} \ \kappa - 2 + \cos\theta \tag{A8}$$

$$u_3 = \frac{2}{\mu}\sqrt{\frac{r}{2\pi}} K_{III} \sin\frac{\theta}{2} \tag{A9}$$

where $\mu$ is the shear modulus and $\kappa$ is the Kosolov constant.

## References


[1]Babuska, I., Melenk, J., "The partition of unity method." *International Journal for Numerical Methods in Engineering,* Vol. 40, 1997, pp. 727-758.

[2]Moës, N., Dolbow, J., Belytschko, T., "A finite element method for crack growth without remeshing." *International Journal for Numerical Methods in Engineering,* Vol. 46, 1999, pp. 131-150.

[3]Gravouil, A., Moës, N., Belytschko, T., "Non-planar 3D crack growth by the extended finite element and level sets - Part II: Level set update." *International Journal for Numerical Methods in Engineering,* Vol. 53, 2002, pp. 2569-2586.

[4]Kassim, A., Topping, B., "Static reanalysis: A review." *Journal of Structural Engineering,* Vol. 113, 1987, pp. 1029-1045.

[5]Wu, B., Li, Z., "Static reanalysis of structres with added degrees of freedom." *Communications in Numerical Methods in Engineering,* Vol. 22, 2006, pp. 269-281.

[6]Wu, B., Lim, C., Li, Z., "A finite element algorithm for reanalysis of structures with added degrees of freedom." *Finite Elements in Analysis and Design,* Vol. 40, 2004, pp. 1791-1801.

[7]Sherman, J., Morisson, W., "Adjustment of an inverse matrix corresponding to a change in one element of a given matrix." *Annals of Mathematical Statistics,* Vol. 21, 1950, pp. 124-127.

[8]Li, Z., Lim, C., Wu, B., "A comparison of several reanalysis methods for structural layout modifications with added degrees of freedom." *Structural and Multidisciplinary Optimization,* Vol. 36, 2008, pp. 403-410.

[9]Osher, S., Sethian, J., "Fronts propagating with curvature dependent speed: Algorithms based on Hamilton-Jacobi formulations." *Journal of Computational Physics,* Vol. 79, 1988, pp. 12-49.

[10]Osher S, F.R., "Level set methods: An overview and some recent results." *Journal of Computational Physics,* Vol. 169, 2001, pp. 463-502.

[11]Stolarska, M., Chopp, D., Moës, N., Belytschko, T., "Modelling crack growth by level sets in the extended finite element method." *International Journal for Numerical Methods in Engineering,* Vol. 51, 2001, pp. 943-960.

[12]Sukumar, N., Chopp, D., Moës, N., Belytschko, T., "Modeling holes and inclusions by level sets in the extended finite-element method." *Computer Methods in Applied Mechanics and Engineering,* Vol. 190, 2001, pp. 6183-6200.

[13]Belytschko, T., Moës, N., Usui, S., Parimi, C., "Arbitrary discontinuities in finite elements." *International Journal for Numerical Methods in Engineering,* Vol. 50, 2001, pp. 993-1013.

[14]Fleming, M., Chu, A., Moran, B., Belytschko, T., "Enriched element-free Galerkin methods for crack tip fields." *International Journal for Numerical Methods in Engineering,* Vol. 40, 1997, pp. 1483-1504.

[15]Belytschko, T., Black, T., "Elastic crack growth in finite elements with minimal remeshing." *International Journal for Numerical Methods in Engineering,* Vol. 45, 1999, pp. 601-620.

[16]Daux, C., N, M., Dolbow, J., Sukumar, N., Belytschko, T., "Arbitrary branched and intersecting cracks with the extended finite element method." *International Journal for Numerical Methods in Engineering*, Vol. 48, 2000, pp. 1741-1760.

[17]Mousavi, S., Xiao, H., Sukumar, N., "Generalized quadrature rules on arbitrary polygons." *International Journal for Numerical Methods in Engineering*, Vol. 00, 2009, pp. 1-26.

[18]Sukumar, N., Prévost, J., "Modeling quasi-static crack growth with the extended finite element method Part I: Computer implementation." *International Journal of Solids and Structures*, Vol. 40, 2003, pp. 7513-7537.

[19]Shih, C., Asaro, R., "Elastic-plastic analysis of cracks on bimaterial interfaces: part I - small scale yielding." *Journal of Applied Mechanics*, Vol. 55, 1988, pp. 299-316.

[20]Paris, P., Gomez, M., Anderson, W., "A rational analytic theory of fatigue." *The Trend in Engineering*, Vol. 13, 1961, pp. 9-14.

[21]Tanaka, K., "Fatigue crack propagation from a crack inclined to the cyclic tension axis." *Engineering Fracture Mechanics*, Vol. 6, 1974, pp. 493-507.

[22]Yau, J., Wang, S., Corten, H., "A mixed-mode crack analysis of isotropic solids using conservation laws of elasticity." *Journal of Applied Mechanics*, Vol. 47, 1980, pp. 335-341.

[23]Westergaard, I., "Bearing pressures and cracks." *Journal of Applied Mechanics, Transactions ASME*, Vol. 61, 1939, pp. A49-A53.

[24]Williams, M., "On the stress distribution at the base of a stationary crack, ." *Journal of Applied Mechanics*, Vol. 24, 1957, pp. 109-114.

[25]Rice, J., "A path integral and the approximate analysis of strain concentration by notches and cracks." *Journal of Applied Mechanics*, Vol. 35, 1968, pp. 379-386.

[26]Chapra, S., Canale, R., *Numerical Methods for Engineers*. 2002, New York: McGraw-Hill.

[27]Mukamai, Y. (ed.), *Stress Intensity Factors Handbook*, Pergamon Press, 1987.

[28]Szabo, B., Babuska, I., *Finite Element Analysis*. 1991, New York: Wiley.